Journal of Science and Technology – Smart Systems and Devices
Volume x, Issue x, Month Year, ppp-ppp

Microgrid Optimization with MILP-based Demand Side Management

Quan Le-Anh, Thanh Trinh-Xuan, Anh Nguyen-Tuan, Vinh Pham-Thanh, Hung Ta-Xuan, Tuyen Nguyen-Duc, Son Tran-Thanh*

School of Electrical and Electronics Engineering,
Hanoi University of Science and Technology, Ha Noi, Vietnam

**Corresponding author email: Son Tran-Thanh@hust.edu.vn*

Abstract

The integration of renewable energy sources in microgrids introduces significant operational challenges due to their intermittent nature and the mismatch between generation and demand patterns. Effective demand response (DR) strategies are crucial for maintaining system stability and economic efficiency, particularly in microgrids with high renewable penetration. This paper presents a comprehensive mixed-integer linear programming (MILP) framework for optimizing DR operations in a microgrid with solar generation and battery storage systems. The framework incorporates load classification, dynamic price thresholding, and multi-period coordination for optimal DR event scheduling. Analysis across seven distinct operational scenarios demonstrates peak load reduction of 5%–10% while achieving energy cost savings ranging from 7.5% to 24.5%. The highest performance was observed in scenarios with high solar generation, where the framework achieved 24.49% energy cost reduction through optimal coordination of renewable resources and DR actions. The results validate the framework's effectiveness in managing diverse operational challenges while maintaining system stability and economic efficiency.

Keywords: Demand response, mixed-integer linear programming, microgrid optimization, renewable energy.

1. Introduction

The transition from traditional centralized power generation based on fossil fuels to prosumer-based distributed generation (DG) enables power systems to operate more effectively, reliably, and economically. This transition, together with the increasing penetration of renewable energy sources, necessitates the development of a new and highly complex system architecture, which can only be realized through the concept of the smart grid. Within the smart grid paradigm, the integration of prosumer-based DG sources with information and communication infrastructure is essential [1].

Energy management, control systems for the smooth integration of DG sources, and the handling of intermittent renewable energy supplies are among the key operational challenges associated with this transformation. To address these issues and enhance the resilience and reliability of power systems during emergency conditions, the concept of microgrids (MGs) has emerged as one of the fundamental components of smart grid architecture [2]. Although various definitions exist, a microgrid is generally defined as a group of interconnected loads and distributed generation units that are coordinated and can be viewed as a single controllable entity by the main grid. A microgrid can operate in two modes: grid-connected and stand-alone [3].

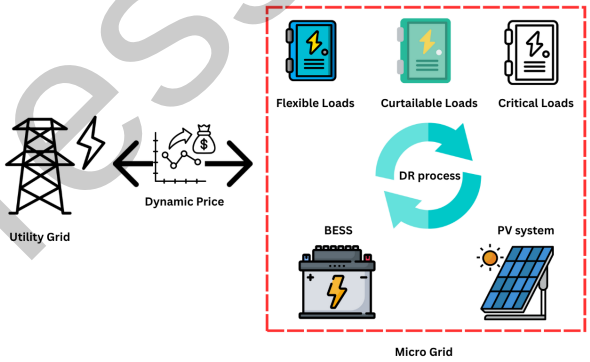

Fig. 1. Integrated PV-BESS microgrid configuration supporting multi-category load demand response

Demand response (DR) is a crucial and effective strategy for encouraging demand-side resources to actively participate in electricity systems with high renewable energy penetration [4]. DR can help maintain the balance between electricity supply and demand, particularly when system security is threatened or when there is a significant amount of renewable energy available for utilization [5]. To assess the impact of consumer participation in DR programs on load profiles, responsive demand economic models must be developed. Such DR program design approaches are likely to enhance customer participation [6]. By considering consumer preferences and behaviors, DR shifts loads from peak to off-peak periods, thereby providing the flexibility required to maximize the

p-ISSN 3093-3285
e-ISSN 3093-3315
https://doi.org/10.51316/jst.xxx.ssad.xxxx.xx.x.x
Received: ...../..../.....; Revised: ...../..../.....;
Accepted: ...../..../.....; Online: ...../..../.....

utilization of renewable energy sources such as wind and solar power, which are most effective during specific hours of the day [7].

Liu *et al.* demonstrated the application of DR programs in a hybrid energy-sharing problem. In their work, a combined heat and power system was proposed that incorporates generation costs, trading costs with the utility grid, electrical and thermal energy trading costs with other microgrids, load characteristics, power consumption utility, and thermal discomfort costs [8]. In [9], the grid is partitioned into multiple self-sufficient microgrids to restore critical loads, with coordination achieved through a mixed-integer linear programming (MILP) optimization framework. Meanwhile, Ali *et al.* addressed operation cost minimization in a grid integrating energy storage systems (ESS) and DR by employing a mixed-integer quadratically constrained programming (MIQCP) approach using the CPLEX solver within the General Algebraic Modeling System (GAMS) [10].

Recent academic contributions have introduced various sophisticated methodologies to enhance microgrid operational efficiency. Specifically, deep learning-based frameworks have been proposed for short-term demand response (DR) operations to navigate the complexities of renewable-based systems [11]. Integrated optimization models now frequently incorporate electric vehicle coordination and adaptive DR strategies to achieve sustainable energy management [12]. Furthermore, research has addressed the challenges of uncertainty in renewable generation and DR programs through robust energy management schemes [13]. Multi-objective frameworks have also been developed to optimize the synergy between hybrid renewable sources and battery energy storage systems [14], while other studies have emphasized the importance of integrating load prioritization with dynamic temporal adaptation to refine system flexibility [15].

Although existing studies have provided valuable insights into DR program optimization, most research efforts treat DR and energy storage management as separate problems. In contrast, this paper proposes an integrated MILP formulation that simultaneously co-optimizes DR operations and battery energy storage system utilization in solar-based microgrids.

The main contributions of this work are summarized as follows:

- Development of an innovative MILP model that incorporates adaptive DR event detection with multi-stage optimization while accounting for time-varying characteristics and system-level constraints.
- Implementation of an improved demand classification and regulation strategy that effectively enhances system operational stability.
- Extensive simulations under diverse operating conditions, demonstrating the model's ability to handle complex system variations while achieving significant cost savings.

The remainder of this paper is organized as follows. Section II presents the proposed methodology and the associated mathematical models. Section III describes the optimization and simulation framework and discusses the results obtained under various operating scenarios. Finally, Section IV concludes the paper and outlines directions for future research.

2. Methodology

2.1. Decision Variables

The optimization considers the following decision variables that represent different aspects of system operation.

Grid power import:

$$P^{l}_{\text{grid}}(t) \geq 0, \quad \forall l \in \mathscr{L}, \forall t \in \mathscr{T}. \tag{1}$$

PV generation across loads:

$$P^{l}_{\text{PV}}(t) \geq 0, \quad \forall l \in \mathscr{L}, \forall t \in \mathscr{T}. \tag{2}$$

BESS operation:

$$P^{\text{ch}}_{\text{BESS}}(t) \geq 0, \quad \forall t \in \mathscr{T}, \tag{3}$$

$$P^{\text{dis}}_{\text{BESS}}(t) \geq 0, \quad \forall t \in \mathscr{T}, \tag{4}$$

$$E^{\text{SOC}}_{\text{BESS}}(t) \geq 0, \quad \forall t \in \mathscr{T}. \tag{5}$$

Demand-side management actions:

$$P^{l}_{\text{shed}}(t) \geq 0, \quad \forall l \in \mathscr{L}_{\text{c}}, \forall t \in \mathscr{T}_{\text{DR}}, \tag{6}$$

$$\begin{aligned} &P^{l}_{\text{shift}}(t_1, t_2) \geq 0, \\ &\forall l \in \mathscr{L}_{\text{f}}, \forall t_1 \in \mathscr{T}_{\text{DR}}, \forall t_2 \in \mathscr{T}_{\text{shift}}. \end{aligned} \tag{7}$$

2.2. Event Trigger

The proposed framework adopts a dual-trigger mechanism, in which demand response (DR) events are initiated when either (i) real-time electricity prices surge or (ii) the system load approaches peak capacity. The total system load is expressed as:

$$\begin{aligned} P^{L}_{\text{total}}(t) = &\sum_{i \in \mathscr{L}_{\text{cr}}} P^{i}_{\text{cr}}(t) + \sum_{j \in \mathscr{L}_{\text{f}}} P^{j}_{\text{f}}(t) \\ &+ \sum_{k \in \mathscr{L}_{\text{c}}} P^{k}_{\text{c}}(t). \end{aligned} \tag{8}$$

Here, $\mathscr{L}_{\text{cr}}$ denotes the set of critical loads, $\mathscr{L}_{\text{f}}$ represents flexible loads, and $\mathscr{L}_{\text{c}}$ corresponds to curtailable loads.

A price-based DR event is triggered when the current grid electricity price exceeds a predefined threshold:

$$\pi_{\text{event}} = \max\big(\alpha\, \pi_{\text{avg}}, \pi_{\text{base}}\big), \tag{9}$$

where α is the price multiplier, π_{avg} is the average electricity price, and π_{base} denotes the base price.

Similarly, a load-based DR event is activated when the real-time total load exceeds a specified limit:

$$P_{\text{event}} = \gamma P_{\text{peak}}, \tag{10}$$

where γ represents the load factor and P_{peak} is the peak load capacity.

2.3. Time Segments

To effectively manage costs and resources, the optimization framework operates on a time-of-use (TOU) basis. This temporal segmentation is crucial for enabling strategic actions:

$$\mathscr{T}_{\text{off-peak}} = [0,5] \cup [22,23], \tag{11}$$

$$\mathscr{T}_{\text{shoulder}} = [6,9] \cup [13,16] \cup [20,21], \tag{12}$$

$$\mathscr{T}_{\text{peak}} = [10,12] \cup [17,19]. \tag{13}$$

2.4. Demand Side Management

The optimization model determines the optimal magnitude of load to curtail during a DR event, subject to a predefined maximum reduction limit:

$$0 \le P^{l}_{\text{shed}}(t) \le \beta_{\max} P^{l}_{\text{c}}(t). \tag{14}$$

where $\beta_{\max}$ is the maximum reduction factor.

Energy conservation in load shifting:

$$\sum_{t_2 \in \mathscr{T}_{\text{shift}}} P^{l}_{\text{shift}}(t_1,t_2)\,\eta_{\text{shift}} = \sum_{t_1 \in \mathscr{T}_{\text{DR}}} P^{l}_{\text{shift}}(t_1,t). \tag{15}$$

The total available DR capacity of the microgrid represents the system's overall flexibility and is a key input for the optimization problem:

$$\text{Cap}_{\max} = \mu \sum_{j \in \mathscr{L}_{\text{f}}} P^{j}_{\text{f}} + \beta_{\max} \sum_{k \in \mathscr{L}_{\text{c}}} P^{k}_{\text{c}}. \tag{16}$$

2.5. BESS System

The Battery Energy Storage System (BESS) is a pivotal component of the microgrid, offering significant operational flexibility. The SOC dynamic relationship is expressed as:

$$E^{\text{SOC}}_{\text{BESS}}(t) = E^{\text{SOC}}_{\text{BESS}}(t-1) + \eta \sum_{l \in \mathscr{L}} P^{\text{ch}}_{\text{BESS}}(t) - \frac{1}{\eta} \sum_{l \in \mathscr{L}} P^{\text{dis}}_{\text{BESS}}(t). \tag{17}$$

SOC limit is:

$$E^{\text{SOC}}_{\min} \le E^{\text{SOC}}_{\text{BESS}}(t) \le E^{\text{SOC}}_{\max}. \tag{18}$$

Power rating constraint:

$$0 \le P^{\text{ch}}_{\text{BESS}}(t),\ P^{\text{dis}}_{\text{BESS}}(t) \le P^{\max}_{\text{BESS}}. \tag{19}$$

Period-specific charging limit:

$$\sum_{l \in \mathscr{L}} P^{\text{ch},l}_{\text{BESS}}(t) \le c_{\text{peak}} P^{b}_{\max}, \quad \forall t \in \mathscr{T}_{\text{peak}}. \tag{20}$$

2.6. PV Source

Solar power allocation must respect available generation:

$$\sum_{l \in \mathscr{L}} P^{l}_{\text{PV}}(t) \le P_{\text{PV,max}}, \quad \forall t \in \mathscr{T}. \tag{21}$$

2.7. Utility Grid

The utility grid serves as the primary source of reliable, dispatchable power for the microgrid:

$$P^{l}_{\text{grid}}(t) \ge 0, \quad \forall l \in \mathscr{L},\ \forall t \in \mathscr{T}. \tag{22}$$

2.8. Operational Constraints

The most fundamental constraint in any power system is the power balance equation:

$$P^{l}_{\text{grid}}(t) + P^{l}_{\text{PV}}(t) + \left(P^{\text{dis}}_{\text{BESS}}(t) - P^{\text{ch}}_{\text{BESS}}(t)\right) = P^{L}_{\text{total}}(t) - P^{l}_{\text{shed}}(t) - \sum_{t_2} P^{l}_{\text{shift}}(t,t_2) + \sum_{t_1} P^{l}_{\text{shift}}(t_1,t). \tag{23}$$

A constraint is added to cap the amount of power that can be imported from the grid during these times:

$$\sum_{l \in \mathscr{L}} P^{l}_{\text{grid}}(t) \le \nu_p P_{\text{peak}}, \quad \forall t \in \mathscr{T}_{\text{peak}}. \tag{24}$$

Minimum load requirements:

$$\sum_{l \in \mathscr{L}} P^{l}_{\text{grid}}(t) \ge \varphi_{\min} \sum_{l \in \mathscr{L}} P^{l}(t), \quad \forall t \in \mathscr{T}. \tag{25}$$

2.9. Objective Function

The goal of the optimization framework is to minimize the total operational cost of the microgrid over the 24-hour horizon:

$$\min C = C_{\text{grid}} + C_{\text{peak}} - C_{\text{DR}} - C_{\text{shift}} + C_{\text{penalty}}. \tag{26}$$

The total expense of importing electricity from the utility grid is calculated by:

$$C_{\text{grid}} = \sum_{t \in \mathscr{T}} \sum_{l \in \mathscr{L}} P^{l}_{\text{grid}}(t)\,\rho(t). \tag{27}$$

This component models the cost associated with this peak demand:

$$C_{\text{peak}} = c_{\text{peak}}\, P_{\text{peak}}. \tag{28}$$

This term quantifies the financial benefit of participating in DR events through load shifting:

$$C_{\text{shift}} = \sum_{l \in \mathscr{L}_{\text{f}}} \sum_{t_1 \in \mathscr{T}_{\text{DR}}} \sum_{t_2 \in \mathscr{T}_{\text{shift}}} B_{\text{shift}}\, P^{l}_{\text{shift}}(t_1,t_2). \tag{29}$$

This component captures the economic advantage of shedding load:

$$C_{\text{DR}} = c_{\text{DR}} \sum_{l \in \mathscr{L}_{\text{c}}} \sum_{t \in \mathscr{T}_{\text{DR}}} P^{l}_{\text{shed}}(t). \tag{30}$$

This final component is added to the objective function to guide the solver towards more practical and stable solutions:

$$\begin{aligned} C_{\text{penalty}} = & \sum_{t \in \mathscr{T}_{\text{peak}}} \omega_{\text{peak}} \left(\sum_{l \in \mathscr{L}} P^{l}_{\text{grid}}(t) \right) \\ & + \sum_{t \in \mathscr{T}} \omega_{\text{penalty}} \left| \sum_{l \in \mathscr{L}} P^{l}_{\text{grid}}(t) \right. \\ & \left. - \sum_{l \in \mathscr{L}} P^{l}_{\text{grid}}(t-1) \right|. \end{aligned} \tag{31}$$

2.10. Limit Constraints

Shifting limit:

$$\sum_{t_2 \in \mathscr{T}_{\text{shift}}} P^{l}_{\text{shift}}(t, t_2) \leq \alpha_{\max} P^{l}_{\text{f}}, \quad \forall l \in \mathscr{L}_{\text{f}}, \forall t \in \mathscr{T}. \tag{32}$$

The peak demand is defined as:

$$P_{\text{peak}} \geq \sum_{l \in \mathscr{L}} P^{l}_{\text{grid}}(t), \quad \forall t \in \mathscr{T}. \tag{33}$$

The change in the import power from the grid is limited by peak load:

$$\begin{aligned} & \left| P^{l}_{\text{grid}}(t) - P^{l}_{\text{grid}}(t-1) \right| \\ & \qquad \leq \gamma_{\text{ramp}} P_{\text{peak}}, \end{aligned} \tag{34}$$

for all $l \in \mathscr{L}$ and $t \in \mathscr{T} \setminus \{0\}$.

3. Simulation and Results

3.1. Simulation Assumptions

To ensure the computational tractability and verifiability of the proposed optimization framework, several simplifying assumptions are established. The model operates on a 24-hour scheduling horizon, utilizing deterministic day-ahead data for load demand, solar generation, and electricity pricing. Throughout the simulation, the microgrid is assumed to remain in a grid-connected state. Furthermore, we consider the load classifications to be predefined and static, while the Battery Energy Storage System (BESS) functions with constant charging and discharging efficiencies within strictly enforced state-of-charge limits. Finally, the framework prioritizes active power balance; as such, detailed AC network constraints—including voltage regulation and line congestion—are omitted to maintain the linearity of the MILP formulation.

3.2. Demand Response Simulation Strategy

The demand response (DR) simulation adopted a two-stage framework comprising (i) DR event detection and (ii) subsequent optimization. Event detection employed dynamic thresholds, with the price threshold defined π_{th} as $\max(1.2\pi_{\text{base}}, \$150/\text{MWh})$ and load threshold P_{th} at 80% of peak demand. The time horizon was segmented into distinct pricing periods as shown in Table 1.

Table 1. Time-of-Use Period Classification

Periods Type	Hours
Off-peak	[0–5], [22–23]
Shoulder	[6–9], [13–16], [20–21]
Peak	[10–12], [17–19]

The DR constraints were specified as follows: a maximum curtailable load fraction of $\alpha_{\max} = 0.2$ and a maximum shifting window for flexible loads $\tau_{max} =$ 12 hours. The flexible load adjustment factor δ_f was set to 0.3, allowing for significant load shifting potential while maintaining system stability.

Table 2. BESS Parameters

BESS1, BESS 2 capacity	1.5 – 1.7 MWh
SOC Limits (E_{min} - E_{max})	15% – 95%
Maximum charging/discharging power rate (P^{max}_{BESS})	0.7 (MW)
Peak Penalty Factor (δ_{peak})	0.5
Efficiency (η)	0.8

The microgrid configuration in this study is established as a representative benchmark model, serving as a strategic research assumption to validate the proposed MILP framework. While the system architecture is a modeled environment designed by the research team, it is driven by validated historical time-series data from the 2014-2015 period, including real-world load profiles and solar irradiance. This approach allows for a controlled and rigorous methodological validation, independent of the site-specific idiosyncrasies of a single field-operational grid. Furthermore, the decision to retain the original U.S. dollar currency and historical pricing structures is a deliberate assumption intended to ensure numerical consistency and eliminate external uncertainties, such as exchange rate volatility or subsequent inflation. Consequently, the effectiveness of the MILP-based strategy is demonstrated through relative percentage improvements in energy costs and peak demand reduction, establishing the model's capability as a generalizable solution for microgrid optimization rather than a site-specific financial estimate.

3.3. Optimization Implementation

The MILP optimization was implemented using GAMS (General Algebraic Modeling System) with the CBC (Coin-or Branch and Cut) solver. The optimization framework incorporated multiple variable sets: grid import $P^{l,t}_{grid}$, solar allocation $P^{s,l,t}_{solar}$, bess operations ($P^{b,l,t}_{ch}, P^{b,l,t}_{dis}, E^{b}_{SOC}(t)$), load reductions $P^{l,t}_{red}$, load shifting $P^{l,t1,t2}_{shift}$. The solver was configured with a 600-second time limit and 1% optimality gap to ensure practical convergence.

3.4. Last Day Analysis and Results

Detailed analysis was performed for September 15, 2015, with system configuration and load distribution shown in Fig.2.

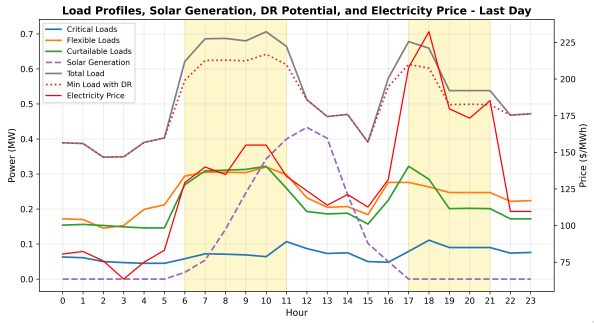

Fig. 2. Data Analysis of 2015-09-15 (Last Day)

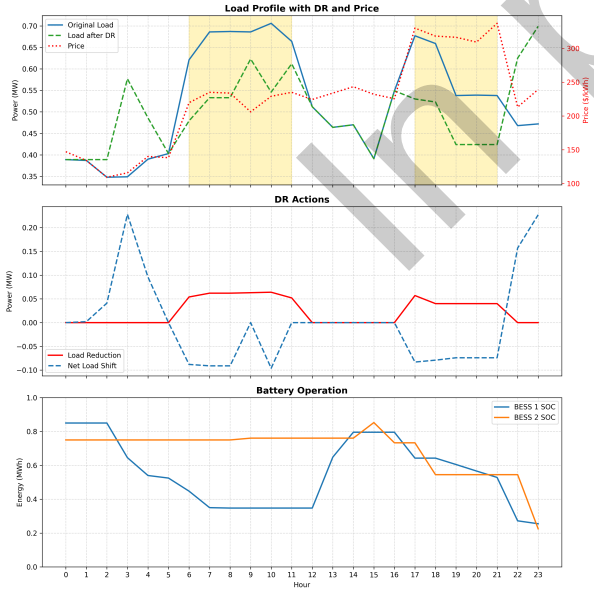

Fig. 3. Optimization Results of 2015-09-15 (Last Day)

The DR event identification algorithm identified 11 critical hours requiring intervention, as illustrated in Fig.2. Two distinct DR periods were identified: a morning period (hours 6-11) with average price \$132.84/MWh and load 0.631 MW, and an evening period (hours 17-21) with higher average price \$195.68/MWh and load 0.59 MW. As shown in Fig. 3, the optimization successfully reduced and shifted loads during these periods, achieving significant peak reduction and cost savings.

Table 3. Last Day - Optimization Results Summary

Metric	Original	Optim.	Improv.
Energy costs (\$)	1199.616	1109.148	7.54%
Peak Charges (\$)	4895.716	4668.02	4.65%
Total Cost (\$)	6874.073	6301.371	8.33%
Peak Load (MW)	0.706	0.67	5.09%
Total Grid (MWh)	9.255	8.624	6.82%

The optimization results are summarized in Table 3, demonstrating substantial improvements across multiple metrics. The total load was reduced from 12.593 MWh to 11.55 MWh through DR strategies. The peak load was reduced from 0.706 MW to 0.67 MW, representing a 5.09% reduction. BESS operations maintained SOC within 20–95%, enabling peak shaving and shifting, with total charge/discharge of 1.446 MWh (BESS 1) and 0.689 MWh (BESS 2). The economic benefits energy costs reduced by 7.541% (from 1,199.616\$ to 1109.148\$) and peak charges decreased by 4.651% (from 4,895.716\$ to 4,668.02\$). Additional benefits of 53.1\$ from DR actions and 38.02\$ from load shifting.

3.5. High Price Day Analysis

Analysis of the high price scenario (March 31, 2015) revealed significant demand response opportunities during periods of elevated electricity prices. As shown in Fig.4 The load profile exhibited one distinct DR

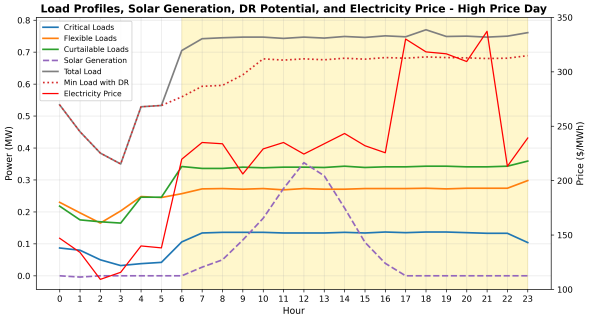

Fig. 4. Data Analysis of 2015-03-31 (High Price Day)

event periods (hours 6–23), with prices reaching \$339.91/MWh during peak periods. The total load of 16.28 MWh was distributed across critical (2.70 MWh), flexible (6.20 MWh), and curtailable loads (7.38 MWh), providing substantial DR potential. The optimization results, illustrated in Fig.5, demonstrate effective load reduction and shifting patterns, particularly during peak price periods.

The battery operation profile shows strategic charging during low-price periods and discharging during high-price intervals, contributing cost savings among all scenarios with 9.874% reduction in energy costs and 11.189% in total costs.

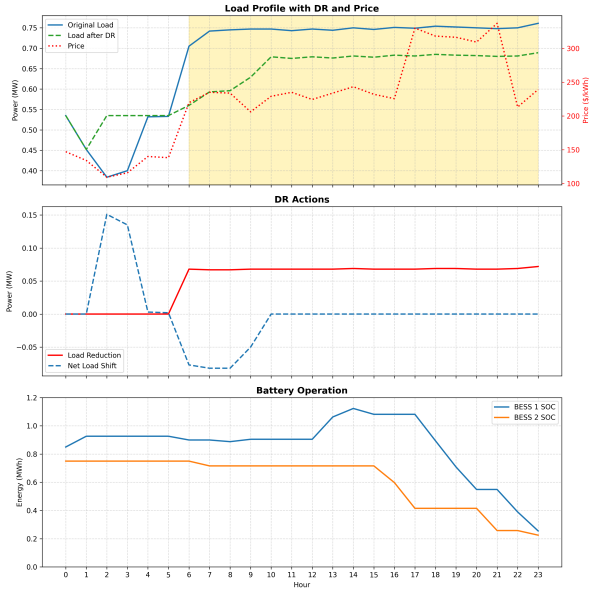

Fig. 5. Optimization Results of 2015-03-31 (High Price Day)

Table 4. Optimization Results Summary (High Price Scenario)

Metric	Original	Optimized	Improvement
Energy Cost ($)	3065.691	2762.973	9.874%
Peak Charges ($)	7041.128	6420.000	8.821%
Total Cost ($)	11387.32	10113.156	11.189%
Peak Grid Load (MW)	0.587	0.535	8.821%
Peak Total Load (MW)	0.761	0.689	9.435%

3.6. High Demand Day Analysis

In the high-demand scenario (December 30, 2014), the system operated under particularly challenging conditions, with very low solar generation (0.068 MWh) and the highest total load (19.27 MWh) recorded among all test cases.

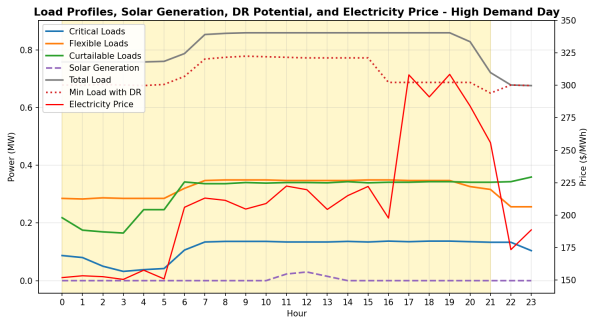

Fig. 6. Data Analysis of 2014-12-30 (High Demand Day)

Fig.6 illustrates the considerable load demand observed across all categories, where flexible and curtailable loads comprise a major share of the overall consumption.

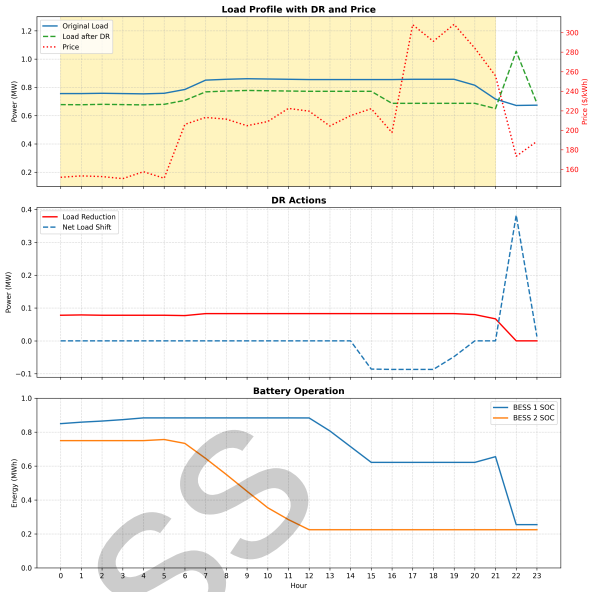

Fig. 7. Optimization Results of 2014-12-30 (High Demand Day)

As shown in Fig.7, the proposed optimization model effectively coordinated demand response operations through synchronized load curtailment and battery dispatch. Even under constrained renewable generation, the system achieved a 9.803% decrease in energy expenditure and a 12.371% reduction in total operating cost, confirming the framework's capability to efficiently manage high-demand operating scenarios.

Due to significant price variations between the 21:00 and 22:00 intervals, the optimization logic shifts consumption, inadvertently creating a secondary load peak that exceeds the original baseline (increasing from 0.861 MW to 1.055 MW). However, this phenomenon is accepted as a strategic trade-off to achieve a substantial 12.37% reduction in the Total Cost.

Table 5. Optimization Results Summary

Metric	Original	Optimized	Improvement
Energy Cost ($)	3844.507	3467.625	9.803%
Peak Charges ($)	9255.627	8240.644	10.966%
Total Cost ($)	14952.39	13102.602	12.371%
Peak Grid Load (MW)	0.771	0.687	10.966%
Peak Total Load (MW)	0.861	1.055	-22.541%

3.7. High Solar - Low Price Analysis and Results

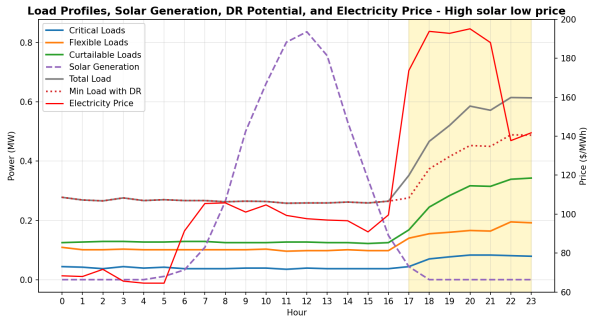

Fig. 8. Data Analysis of 2015-08-19 (High Solar Low Price)

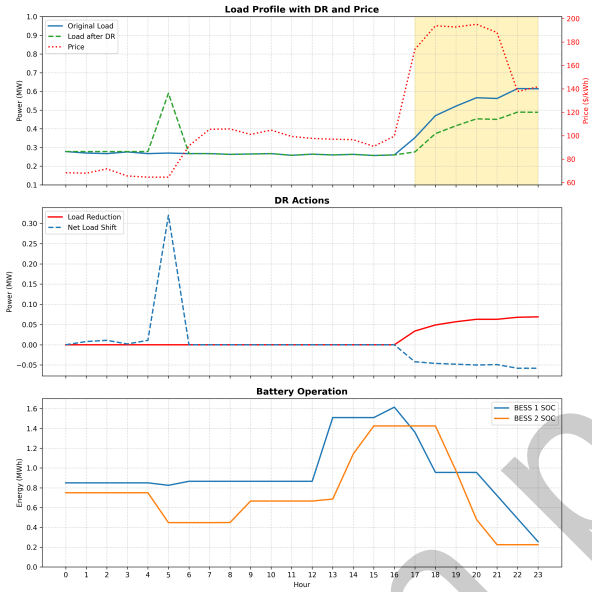

Fig. 9. Optimization Results of 2015-08-19 (High Solar Low Price)

Table 6. Optimization Results Summary (High Solar Scenario)

Metric	Original	Optimized	Improvement
Energy Cost ($)	419.979	317.096	24.497%
Total Cost ($)	3838.893	3576.896	6.825%
Peak Charges ($)	3336.0	3336.0	0%
Peak Grid Load (MW)	0.278	0.278	0%
Peak Total Load (MW)	0.615	0.590	4.130%

The high solar–low price scenario (August 19, 2015) demonstrated the effectiveness of the proposed framework in enhancing renewable energy utilization. As shown in Fig.8, a significant solar generation output of 5.05 MWh coincided with relatively low market prices. The corresponding load profile indicates the efficient integration of solar energy, particularly during midday periods. The optimization outcomes, presented in Fig.9, reveal the strategic shifting of demand toward intervals with high solar availability, resulting in the highest energy cost reduction of 24.497% through the coordinated management of renewable generation and demand response activities.

3.8. Low Solar – High Price Analysis and Results

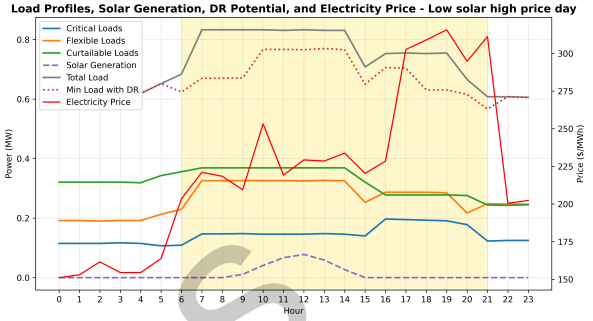

Fig. 10. Data Analysis of 2015-02-06 (Low Solar High Price)

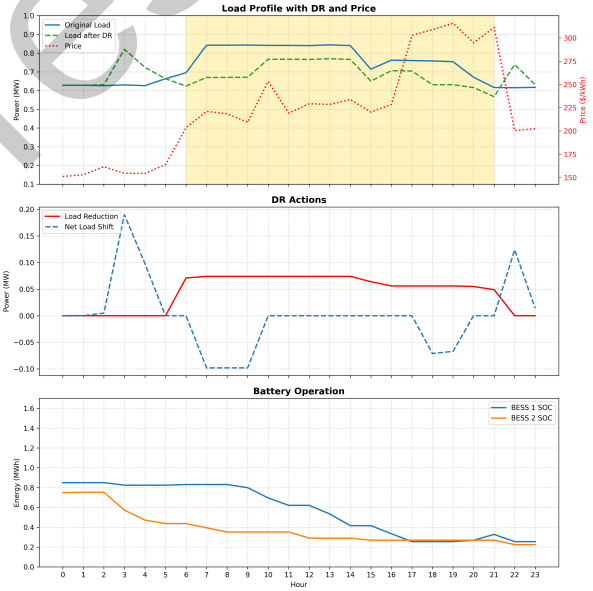

Fig. 11. Optimization Results of 2015-02-06 (Low Solar High Price)

The low solar–high price scenario (February 6, 2015) evaluated the robustness of the proposed framework under limited renewable generation (0.283 MWh) and elevated electricity prices. As illustrated in Fig.10, the solar output was notably low compared to the substantial system demand of 17.291 MWh. The optimization outcomes, presented in Fig.11, demonstrate the efficient scheduling of DR events across 15 critical hours, achieving a 6.64% reduction in energy cost despite adverse operating conditions. The BESS operation

strategy emphasized peak shaving and price arbitrage to offset the limited solar contribution and maintain cost efficiency.

Table 7. Optimization Results Summary (Low Solar–High Price Scenario)

Metric	Original	Optimized	Improvement
Energy Cost ($)	3609.590	3369.901	6.640%
Peak Charges ($)	8259.035	7573.662	8.298%
Total Cost ($)	13521.78	12298.501	9.047%
Peak Grid Load (MW)	0.688	0.631	8.298%
Peak Total Load (MW)	0.844	0.820	2.789%

3.9. Synthesis of Cross-Scenario Robustness

The comprehensive evaluation across seven distinct operational scenarios validates the operational robustness of the proposed MILP-based day-ahead scheduling framework. Despite significant fluctuations in solar availability, extreme price volatility, and high-demand stress—such as the conditions simulated in the high-demand and high-price scenarios—the optimization consistently yielded feasible dispatch solutions while strictly maintaining the BESS state-of-charge within the operational limits of 20–95%. These findings demonstrate that the coordinated PV-BESS-DR approach provides a resilient energy management strategy, effectively balancing supply and demand to achieve consistent techno-economic improvements. However, as this framework is formulated at the energy-management and scheduling level, these results should be interpreted as evidence of operational feasibility and robustness rather than transient, small-signal, or voltage stability. Nevertheless, the results confirm the framework's effectiveness in ensuring economic efficiency and system-level reliability for grid-connected microgrids under diverse environmental and market conditions.

4. Conclusion

This paper proposed a mixed-integer linear programming (MILP) framework for coordinated demand response (DR) optimization in microgrids with solar photovoltaic (PV) and battery energy storage systems (BESS). The model jointly optimizes load shedding, rescheduling, and storage utilization to ensure operational reliability and economic efficiency. By integrating dynamic pricing, multi-period coordination, and load classification, the framework provides a unified approach for managing renewable variability and demand-side flexibility.

Simulation studies conducted across seven operating scenarios validated the robustness of the proposed framework. The results demonstrated consistent improvements in system performance, including up to a 10% reduction in peak demand and a 24.49% decrease in energy costs under high solar generation. Coordinated control between DR and BESS effectively enabled peak shaving, load shifting, and price arbitrage while maintaining the stability of critical loads and maximizing overall system flexibility.

Despite the demonstrated benefits, it is essential to recognize the limitations of the proposed framework for practical smart-grid applications. As a deterministic day-ahead MILP optimization, the system's performance is inherently dependent on the quality and accuracy of forecasting inputs for load demand and renewable generation. Furthermore, the current model does not explicitly incorporate complex physical and technical factors, such as battery degradation, communication latencies, or high-fidelity converter and network dynamics. Additionally, the computational burden may increase significantly when introducing finer time resolutions, a larger number of controllable assets, or comprehensive network-constrained formulations. These points distinguish the present energy management framework from a full online operational deployment and establish a clear boundary for its current practical implementation.

Future work will focus on integrating advanced forecasting techniques for solar generation and demand prediction to enhance real-time optimization accuracy. The adoption of distributed and hierarchical optimization methods will also be explored to improve scalability for large-scale and networked microgrids. Moreover, incorporating machine learning-based adaptive pricing and risk-aware control strategies is expected to further strengthen system resilience and economic performance. Finally, the optimization model will be recalibrated to incorporate contemporary regional tariff structures, such as the Vietnamese electricity pricing system, to enhance the framework's practical applicability and alignment with local energy markets.

5. Acknowledgement

This research is funded by Hanoi University of Science and Technology (HUST) under project number T2024-T-014.

References

[1] K. D. Mistry and R. Roy, Enhancement of loading capacity of distribution system through distributed generator placement considering techno-economic benefits with load growth, International Journal of Electrical Power & Energy Systems, vol. 54, pp. 505–515, Jan. 2014. https://doi.org/10.1016/j.ijepes.2013.07.032

[2] M. H. Hemmatpour, M. Mohammadian, and A. A. Gharaveisi, Optimum islanded microgrid reconfiguration based on maximization of system loadability and minimization of power losses, International Journal of Electrical Power & Energy Systems, vol. 78, pp. 343–355, Jun. 2016.
https://doi.org/10.1016/j.ijepes.2015.11.040

[3] D. E. Olivares, C. A. Cañizares, and M. Kazerani, A Centralized energy management system for isolated microgrids, IEEE Trans. Smart Grid, vol. 5, iss. 4, pp. 1864–1875, Apr. 2014.
https://doi.org/10.1109/TSG.2013.2294187

[4] G. Strbac, Demand side management: Benefits and challenges, Energy Policy, vol. 36, iss. 12, pp. 4419–4426, Dec. 2008.
https://doi.org/10.1016/j.enpol.2008.09.030.

[5] J. Wang, H. Zhong, Z. Ma, Q. Xia, and C. Kang, Review and prospect of integrated demand response in the multi-energy system, Appl. Energy, vol. 202, pp. 772–782, Sep. 2017.
https://doi.org/10.1016/j.apenergy.2017.05.150

[6] H. A. Aalami, M. P. Moghaddam, and G. R. Yousefi, Demand response modeling considering Interruptible/Curtailable loads and capacity market programs, Appl. Energy, vol. 87, no. 1, pp. 243–250, Jan. 2010.
https://doi.org/10.1016/j.apenergy.2009.05.041

[7] M. Kermani, E. Shirdare, A. Najafi, B. Adelmanesh, D. L. Carnì, and L. Martirano, Optimal self-scheduling of a real energy hub considering local DG units and demand response under uncertainties, IEEE Trans. Ind. Appl. vol. 57, iss. 4, pp. 3396–3405, Apr. 2021.
https://doi.org/10.1109/TIA.2021.3072022

[8] N. Liu, J. Wang, and L. Wang, Hybrid energy sharing for multiple microgrids in an integrated heat–electricity energy system, IEEE Trans. Sustain. Energy, vol. 10, iss. 3, pp. 1139–1151, Aug. 2019.
https://doi.org/10.1109/TSTE.2018.2861986

[9] M. Ott, M. AlMuhaini, and M. Khalid, A MILP-based restoration technique for multi-microgrid distribution systems, IEEE Access, vol. 7, pp. 136801–136811, Sep. 2019.
https://doi.org/10.1109/ACCESS.2019.2942633

[10] M. Ali, M. A. Abdulgalil, I. Habiballah, and M. Khalid, Optimal scheduling of isolated microgrids with hybrid renewables and energy storage systems considering demand response, IEEE Access, vol. 11, pp. 80266–80273, Jul. 2023.
https://doi.org/10.1109/ACCESS.2023.3296540

[11] S. S. Gharehveran, K. Shirini, S. C. Khavar, S. H. Mousavi, and A. Abdolahi, Deep learning-based demand response for short-term operation of renewable-based microgrids, The Journal of Supercomputing, vol. 80, pp. 26002–26035, Aug. 2024.
https://doi.org/10.1007/s11227-024-06407-z

[12] Y. Liu and F. Wan, Integrated optimization of microgrids with renewable energy, electric vehicles, and adaptive demand response for sustainable and efficient energy management, Smart Grids and Sustainable Energy, vol. 10, p. 30, Apr. 2025.
https://doi.org/10.1007/s40866-025-00257-1

[13] S. Ray, A. M. Ali, T. Eshchanov, and E. Khudoynazarov, Optimal energy management of the smart microgrid considering uncertainty of renewable energy sources and demand response programs, Operations Research Forum, vol. 6, p. 53, Apr. 2025.
https://doi.org/10.1007/s43069-025-00450-z

[14] M. Sasikumar, S. Seenivasan, P. Vijayakumar, and S. Manikandan, Multi-objective energy management in microgrids with hybrid renewable energy sources and battery energy storage systems using hybrid optimization algorithm, Transactions on Electrical and Electronic Materials, vol. 27, iss. 3, Oct. 2025.
https://doi.org/10.1007/s42341-025-00673-1

[15] T. Z. Pan, J. Hou, Z. Y. Wang, and W. Hao, Enhanced Microgrid Energy Optimization: Integrating Load Prioritization and Dynamic Temporal Adaptation, Journal of Electrical Engineering & Technology, 2024.
https://doi.org/10.1007/s42835-024-02054-9